PHYSICAL REVIEW B **95**, 060413(R) (2017)

Resonating valence bond states with trimer motifs

Hyunyong Lee,[1,2] Yun-tak Oh,[1] Jung Hoon Han,[1,*] and Hosho Katsura[3,†]
[1]*Department of Physics, Sungkyunkwan University, Suwon 16419, Korea*
[2]*Institute for Solid State Physics, University of Tokyo, Kashiwa, Chiba 277-8581, Japan*
[3]*Department of Physics, Graduate School of Science, The University of Tokyo, Hongo, Bunkyo-ku, Tokyo 113-0033, Japan*
(Received 27 December 2016; published 21 February 2017)

A trimer resonating valence bond (tRVB) state consisting of an equal-weight superposition of trimer coverings on a square lattice is proposed. A model Hamiltonian of the Rokhsar-Kivelson type for which the tRVB becomes the exact ground state is written. The state is shown to have 9^g topological degeneracy on a genus g surface and support $\mathbb{Z}_3$ vortex excitations. Correlation functions show exponential behavior with a very short correlation length consistent with the gapped spectrum. The classical problem of the degeneracy of trimer configurations is investigated by the transfer matrix method.

DOI: 10.1103/PhysRevB.95.060413

Resonating valence bond (RVB) wave functions have been a paradigmatic expression of strongly correlated states of matter, with potential bearings on high-T_c cuprates and two-dimensional spin-liquid materials [1,2]. The basic building block of RVB is the spin singlet pair, also known as the dimer, made out of two constituent $S = \frac{1}{2}$ spins. In the insulating state without holes, every site is covered by one and only one dimer in a particular fashion, which we denote as $|\mathcal{D}\rangle$, the dimer covering. Quantum fluctuation introduces mixing among various dimer coverings, leading to the RVB wave function as the linear superposition of all possible dimer coverings of the lattice, $|\mathrm{RVB}\rangle = \sum_{\mathcal{D}} A_{\mathcal{D}}|\mathcal{D}\rangle$, with amplitude $A_{\mathcal{D}}$. Short-range RVB wave functions of the Rokhsar-Kivelson (RK) type allow dimers over the nearest neighbors only and have been extensively investigated on square [3], triangular [4,5], hexagonal [6], and kagome lattices [7]. More recently it became apparent that the tensor network approach is another potent way to probe short-range RVB physics [8–12].

Works on RVB have been overwhelmingly focused on $S = \frac{1}{2}$ spins, motivated at first by its potential relevance to the cuprate physics and later by the discovery of several two-dimensional spin-liquid materials all formed out of $S = \frac{1}{2}$ constituent spins [13]. The discovery of the spin-liquid phase in the pnictide family of superconductors in recent years [14] has nudged the tide, and now there are active discussions of possible spin-liquid phases realized in various frustrated $S = 1$ spin models [12,15,16]. A pair of spin-1 constituents can form a dimer just as a pair of spin-$\frac{1}{2}$'s does, but there is also a more novel possibility of the trimer, made of three constituent spin-1's forming a spin singlet. The examination of the RVB wave function consisting of trimer motifs, rather than dimers, is the thrust of this Rapid Communication.

The physics of RVB is related to the problem of dimer coverings on planar lattices dating back to the 1930's [17,18] and invigorated by their exact solutions found in 1961 by Kasteleyn [19], and Fisher and Temperley [20]. The combinatorial problem of counting the number of coverings can be rephrased as the evaluation of certain partition functions of classical statistical mechanics models. In turn, this partition function can be written as the tensor trace of judiciously chosen site tensors [21]. The trimer covering problem is the simplest example of generalization of the heavily studied dimer problem. Our strategy is to revisit some known results on the classical trimer covering problem [22–25], generalize them, and use those results to shed light on the quantum superposition of the trimer coverings which we call the trimer RVB state. We argue, in various ways, that low-energy excitations of the trimer RVB are likely to be described by some sort of $\mathbb{Z}_3$ gauge theory with 9^g topological degeneracy on the genus g surface.

Different facets of the trimer covering on the two-dimensional square lattice have been investigated for some time [22–25]. Trimers come in two types: the linear trimer (L type) which extends either horizontally or vertically over three consecutive lattice sites, or the bent trimer (B type) extending over a site and its two nearest neighbors, as illustrated in Fig. 1(k). In this Rapid Communication we consider the square lattice only. Counting the L-trimer covering on a square lattice was done in Ref. [24], and that of the B-type trimer in Ref. [25]. Oddly, the counting problem for the mixed case with both types of trimers allowed has yet to be solved. The mixed trimer problem, to which the L- and B-type cases belong as special limits, can be formulated using the tensor network language [21].

To this end, a site tensor A_{lrud} having a value 1 for the ten configurations shown in Figs. 1(a)–1(j) and zero otherwise is introduced. The indices l,r,u,d refer to left, right, up, and down bonds around each site and take only three possible values 0, 1, and 2. The index $l = 0$ implies the absence of a trimer in that direction. Two independent values 1 and 2 are introduced for the index designating the presence of a trimer bond. As a result, configuration (a) in Fig. 1 cannot be contracted with (c), nor (b) with (d), to form a dimer. Inspection of the index assignments in Fig. 1 should convince the readers that only trimer configurations are allowed under the tensor contraction. L-trimers are formed by contracting (a)-(i)-(c) tensors horizontally, or (b)-(j)-(d) tensors vertically. There are four orientations for B-trimers, each realized by (d)-(e)-(c), (a)-(f)-(d), (a)-(g)-(b), and (c)-(h)-(b) contractions, respectively. A trimer model consisting of L-trimers is only achieved as the limit where (e)-(h) configurations are given the value 0. The B-trimer-only model is the limit with (i) and (j) configurations set to zero. Carrying out a tensor contraction

*hanjh@skku.edu
†katsura@phys.s.u-tokyo.ac.jp

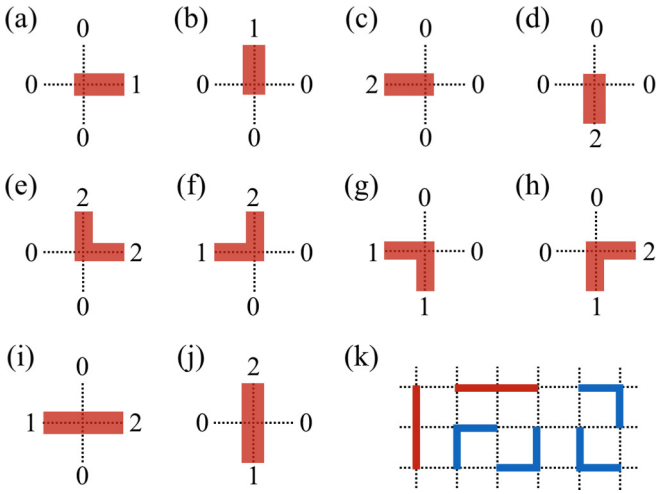

FIG. 1. (a)–(j) Ten possible configurations of a local tensor to realize the trimer covering. Known trimer coverings consisting of linear and bent types only arise as special limits. The numbers 0, 1, and 2 denote the indices of the site tensor. (k) Red and blue bars represent all possible L- and B-type trimers, respectively.

$Z = \sum_{\{l_i,r_i,u_i,d_i\}} A_{l_1 r_1 u_1 d_1} \delta_{r_1 l_2} A_{l_2 r_2 u_2 d_2} \cdots$ gives the number of trimer coverings.

The efficient calculation of Z proceeds on a cylinder geometry with the periodic boundary condition (PBC) imposed along the x direction of length N_x and open ends along the y direction of length N_y. The largest eigenvalue λ of the row-to-row transfer matrix (TM) is used to evaluate $Z \sim \lambda^{N_y}$. The entropy per site is $s = \ln Z/N$, where $N = N_x N_y$ counts the number of lattice sites. We quote below the thermodynamic extrapolation of the entropy for the mixed (both L- and B-type) trimer case along with known results for L-only and B-only types [24,25]:

$$s_\infty = \begin{cases} 0.15852(1.17178) & \text{for L-type,} \\ 0.27693(1.31907) & \text{for B-type,} \\ 0.41194(1.50974) & \text{for L- and B-type.} \end{cases} \quad (1)$$

The number in the parentheses is $x = e^{s_\infty}$, with which one obtains $Z \sim x^N$.

Interestingly, we have found from analysis of the adjacency graph of the transfer matrix that trimer configurations on the cylinder can be classified into three distinct topological sectors [26]. The winding number characterizing each sector can be defined with a string threading the dual lattice. As depicted in Fig. 2(a), we assign a direction to the string and give a weight $\omega = e^{2\pi i/3}$ when the center position of the trimer is seen on the right side of the path, and ω^* if seen on the left side. With this definition, the total weight for the elementary string loop surrounding a site anticlockwise [Fig. 2(b)] is always ω, and it can be considered as a locally conserved quantity in the trimer problem. The winding number Γ around a single trimer is the product of three factors of ω as the loop should consist of three consecutive elementary loops, thus giving $\Gamma = \omega^3 = 1$. For noncontractible loops defined on a compact manifold such as the torus, the allowed winding numbers are $\Gamma = 1, \omega, \omega^*$, as readers can easily verify, and cannot be modified by local rearrangements of the string or of the trimers.

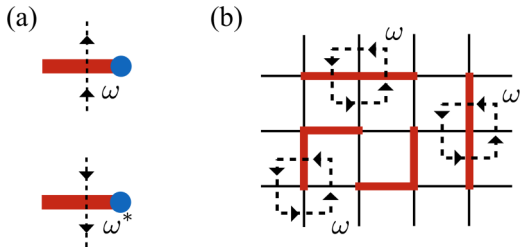

FIG. 2. (a) Assignment of the weight $\omega = e^{2\pi i/3}$ and its conjugate ω^* for the passage through the dual lattice with the center of the trimer (blue dot) on the right and left side of the path, respectively. (b) For any elementary loop surrounding a site, the total weight is always $\Gamma = \omega$. For any loop surrounding a single trimer, the total weight is $\Gamma = \omega^3 = 1$.

A quantum Hamiltonian with 9^g (g = genus of the manifold) topological degeneracy may be constructed in analogy with the RK Hamiltonian [3,4]:

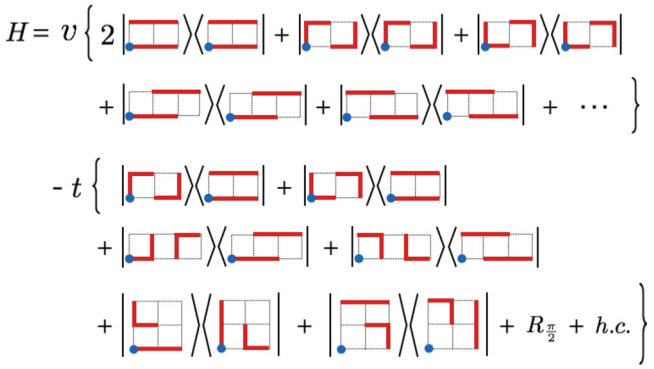

(2)

The summation over all lattice translations of the blue-dot site, as well as the 90° rotation ($R_{\frac{\pi}{2}}$) of the displayed terms, are assumed. The v and t terms are the potential and resonating pieces, respectively, in analogy with the structure of the RK Hamiltonian for dimers [3,4]. In the potential terms, $\cdots$ denotes all other possible diagonal terms [26]. Resonating terms involve only two trimers at one time and are not able to alter the topological sector of the initial configuration. As with all dimer models, there are certain "staggered states" that cannot be reached by applying any number of resonance moves. An example is given in Fig. 3(a). Acting with the Hamiltonian on the staggered state gives 0 irrespective of t and v values. Higher-order moves such as the simultaneous rearrangement of six trimers caged inside the blue contour in

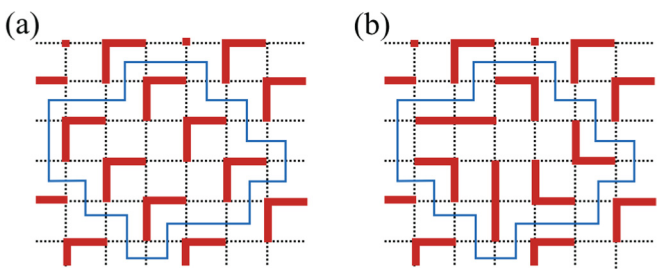

FIG. 3. (a) Staggered trimer configuration. A nonflippable six-trimer block inside the blue boundary can be connected to (b) a flippable configuration through six-trimer resonance moves.

Figs. 3(a) and 3(b) can connect such staggered configurations to flippable ones. Even this six-trimer flip is not able to alter the topological sector.

At $t = v$, the trimer Hamiltonian in Eq. (2) can be recast as a sum of projectors that locally project out the linear superposition of flippable configurations [3,4,26]. Its ground state is the linear superposition of all but the staggered trimer configurations (to be defined shortly), with equal amplitudes, i.e., the trimer resonating valence bond (tRVB) state, $|\text{tRVB}\rangle = \sum_{\mathcal{T}} |\mathcal{T}\rangle$. Here, $|\mathcal{T}\rangle$ refers to a trimer covering within a particular topological sector. For a torus with genus number $g = 1$, we have $9^g = 9$ degenerate ground states not connected with each other by resonance moves of the Hamiltonian. Each one is a unique ground state of the trimer RK Hamiltonian at $t = v$, within the subspace that excludes staggered configurations, due to the Perron-Frobenius theorem [27]. The staggered states also have zero energy, in apparent degeneracy with the tRVB state $|\text{tRVB}\rangle$. One can rule out staggered states from the ground state by perturbing away from the RK point to $v = t - \epsilon$ infinitesimally, $\epsilon/t \ll 1$ [28]. Also, since this perturbation does not mix different topological sectors, we still have 9^g independent ground states.

Connected trimer ($\langle \text{tRVB}|T_i T_j|\text{tRVB}\rangle_c$) and trimer-trimer ($\langle \text{tRVB}|T_i T_{i+\hat{x}} T_j T_{j+\hat{x}}|\text{tRVB}\rangle_c$) correlation functions, where T_i is either an L- or a B-type trimer projector, are evaluated and presented in Fig. 4. By performing a finite size scaling, we obtained very nicely converged values and therefore the results in Fig. 4 are not certainly affected by the finite size effect. All functions decay exponentially with very short correlation lengths of order one lattice spacing, as observed in the dimer

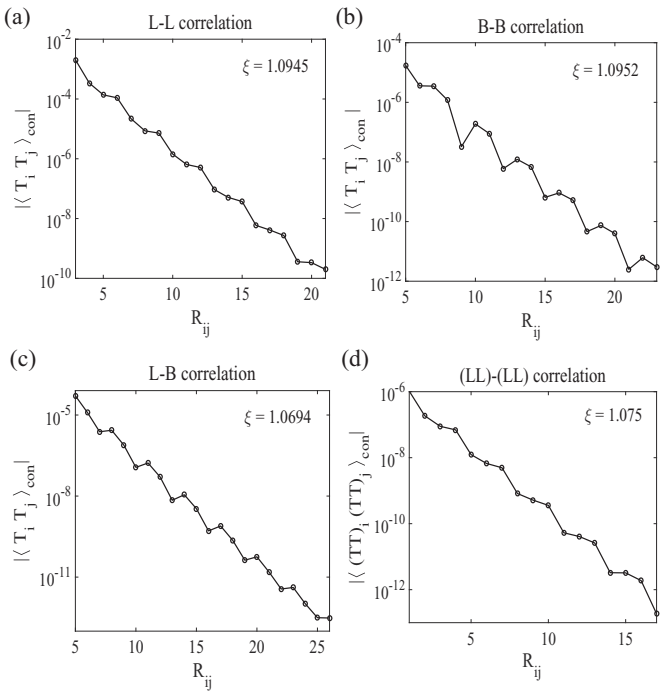

FIG. 4. Correlations between (a) L-type, (b) B-type, (c) L- and B-type, and (d) (LL)-trimers are measured on a 120×120 lattice with the open boundary condition. Here, R_{ij} is the distance between two trimers at the site i and j, and the estimated correlation length ξ is shown for each plot.

RK wave function on the triangular lattice [29,30]. It strongly suggests that the quantum trimer Hamiltonian in Eq. (2) is gapped at the RK point.

The 9^g-fold topological degeneracy along with the likely gapped nature of the ground state suggests a $\mathbb{Z}_3$ gauge theory description of the low-energy dynamics for the trimer Hamiltonian. The relevant magnetic excitations (so-called vortex and antivortex) will also be of $\mathbb{Z}_3$ character, differentiating a vortex from the antivortex [31]. (In the $\mathbb{Z}_2$ gauge theory, vortex and antivortex are the same [32].) A vortex-antivortex pair excitation can be constructed explicitly. Let us consider the same string operator, used previously for defining the winding number, connecting two sites (p_1, p_2) on the dual lattice and define a quantum state

$$|v_1 \bar{v}_2\rangle = \sum_{\mathcal{T}} \omega^{n_r - n_l} |\mathcal{T}\rangle, \tag{3}$$

where $n_{r(l)}$ denotes the number of the trimers crossed by the string from the right (left) side of its center. This state is orthogonal to the ground state in the thermodynamic limit,

$$\langle v_1 \bar{v}_2 | \text{tRVB}\rangle = \sum_{\mathcal{T}} \omega^{n_l - n_r} \propto 1 + \omega + \omega^* = 0. \tag{4}$$

The first equality follows from the assumed orthogonality of different trimer configurations $\langle \mathcal{T}'|\mathcal{T}\rangle = \delta_{\mathcal{T}\mathcal{T}'}$. For a sufficiently large sample and a well-separated vortex-antivortex pair there should be equal numbers of configurations having $n_l - n_r = 0,1,2 \pmod 3$, hence the overlap must be zero. The phase $V_{12} = \omega^{n_l - n_r}$ is topologically identical to the operator creating the $\mathbb{Z}_3$ vortex-antivortex pair in the $\mathbb{Z}_3$ gauge theory [31]. Therefore, $|\text{tRVB}\rangle$ and $|v_1 \bar{v}_2\rangle$ can be considered as a vacuum and a single vortex-antivortex pair state, respectively. In this sense, we may interpret the nontrivial phase ω obtained by the elementary loop in Fig. 2(b) as a result of braiding between the vortex (or antivortex) and a $\mathbb{Z}_3$ charge placed at each site [31].

The $t = v$ RK point defines the first-order phase boundary [4]. For $v/t > 1$, the ground state is one of the staggered configurations such as that shown in Fig. 3(a), defined as states that are annihilated identically by the actions of t and v terms in the trimer Hamiltonian. Any trimer configuration containing a flippable block gains a positive energy $(v - t)n_{\text{fl}}$, where n_{fl} is the number of such flippable blocks. At $v/t = -\infty$, the ground state will be chosen to maximize the number of flippable configurations. It is one of the columnar configurations depicted in Fig. 5, and those are sixfold degenerate at most, depending on the boundary condition and the system size. A likely phase diagram of the quantum trimer model is schematically proposed in Fig. 5. An extensive numerical work

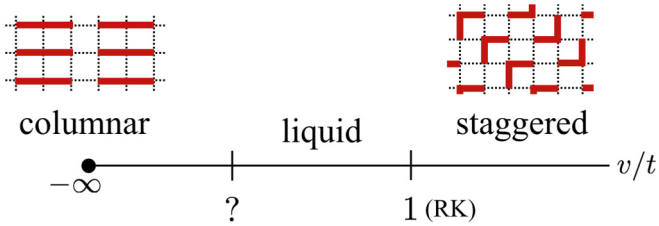

FIG. 5. Schematic phase diagram of the quantum trimer Hamiltonian.

required to identify the phases and phase boundaries between the trimer RVB state at $v/t = 1$ and the columnar phase at $v/t = -\infty$ will be done elsewhere.

The number of staggered configurations in the trimer model grows at least exponentially in the linear dimension. For instance, taking the particular staggered configuration in Fig. 3(a) and reversing all the B-trimer orientations along one of the north-by-west diagonal lines produces another staggered state. That is already 2^{N_d} distinct staggered states where N_d counts the number of diagonal rows in the lattice. This is a much bigger number than the linear growth of staggered states in the square-lattice dimer model [3] or the constant number in the triangular lattice dimer problem [4]. Fortunately, the staggered configurations of the trimer are not allowed in a finite rectangular sample, and therefore the correlation functions shown in Fig. 4 have been measured in an exact $|\mathrm{tRVB}\rangle$.

The trimer RVB state is likely to find a physical context in the frustrated spin-1 model on a square lattice. A sufficiently strong diagonal antiferromagnetic exchange interaction $J_2 > 0$ in addition to the Heisenberg exchange J_1 across the nearest neighbors of the square lattice could favor the formation of a singlet among the three adjacent spins. There is gathering evidence of a spin-liquid phase in the J_1-J_2 frustrated spin-1 model. A recent tensor network analysis of possible $S = 1$ symmetric spin-liquid phases by some of the present authors has found a regime in which the spin-1 RVB states can be realized [12]. A careful inspection of the tensor wave function for the spin-1 RVB revealed that the underlying motifs are a mixture of both spin dimers and spin trimers [12].

A final thought on the possible gauge theory description of the trimer dynamics is in order. We know that the constraint of having one and only one dimer per site translates into the Gauss' law constraint on physically allowed states in the gauge description [33]. The corresponding constraint for the trimer configuration can be derived with the winding number for an elementary dual-lattice plaquette around each site Γ being ω, as discussed earlier. Readers can verify that only the configurations with each site covered by no more than one trimer satisfy this constraint exactly. It seems we have sufficient ingredients regarding the trimer RVB states to declare its candidacy for an example of a $\mathbb{Z}_3$ spin liquid. Much more numerical work will be required to prove the claim quantitatively. In the meantime, it is rather interesting to speculate that a physical example of a $\mathbb{Z}_3$ spin liquid can be written down in terms of a simple generalization of the well-known dimer model.

We learned a great deal on the relation of the dimer/trimer covering problem to tensor networks from Tomotoshi Nishino's insightful lecture given at ISSP in 2016. H.K. was supported in part by JSPS KAKENHI Grants No. JP15K17719 and No. JP16H00985. Y.-T.O. was supported by the Global Ph.D. Fellowship Program through the National Research Foundation of Korea (NRF) funded by the Ministry of Education (No. NRF-2014H1A2A1018320). This research was partially supported by MEXT as "Exploratory Challenge on Post-K computer" (Frontiers of Basic Science: Challenging the Limits).

[1] P. W. Anderson, Science **235**, 1196 (1987).
[2] P. W. Anderson, P. Lee, M. Randeria, T. Rice, N. Trivedi, and F. Zhang, J. Phys.: Condens. Matter **16**, R755 (2004).
[3] D. S. Rokhsar and S. A. Kivelson, Phys. Rev. Lett. **61**, 2376 (1988).
[4] R. Moessner and S. L. Sondhi, Phys. Rev. Lett. **86**, 1881 (2001).
[5] D. A. Ivanov, Phys. Rev. B **70**, 094430 (2004).
[6] H. Yao and S. A. Kivelson, Phys. Rev. Lett. **108**, 247206 (2012).
[7] G. Misguich, D. Serban, and V. Pasquier, Phys. Rev. Lett. **89**, 137202 (2002).
[8] N. Schuch, D. Poilblanc, J. I. Cirac, and D. Pérez-García, Phys. Rev. B **86**, 115108 (2012).
[9] D. Poilblanc, N. Schuch, D. Pérez-García, and J. I. Cirac, Phys. Rev. B **86**, 014404 (2012).
[10] D. Poilblanc and N. Schuch, Phys. Rev. B **87**, 140407 (2013).
[11] D. Poilblanc, P. Corboz, N. Schuch, and J. I. Cirac, Phys. Rev. B **89**, 241106 (2014).
[12] H. Lee and J. H. Han, Phys. Rev. B **94**, 115150 (2016).
[13] L. Balents, Nature (London) **464**, 199 (2010).
[14] F. Wang, S. A. Kivelson, and D.-H. Lee, Nat. Phys. **11**, 959 (2015).
[15] H. C. Jiang, F. Krüger, J. E. Moore, D. N. Sheng, J. Zaanen, and Z. Y. Weng, Phys. Rev. B **79**, 174409 (2009).
[16] H.-C. Jiang, H. Yao, and L. Balents, Phys. Rev. B **86**, 024424 (2012).
[17] R. Fowler and G. Rushbrooke, Trans. Faraday Soc. **33**, 1272 (1937).
[18] T. S. Chang, Proc. R. Soc. London, Ser. A **169**, 512 (1939).
[19] P. Kasteleyn, Physica **27**, 1209 (1961).
[20] H. N. V. Temperley and M. E. Fisher, Philos. Mag. **6**, 1061 (1961).
[21] E. H. Lieb, J. Math. Phys. **8**, 2339 (1967).
[22] J. Van Craen, J. Chem. Phys. **63**, 2591 (1975).
[23] R. Kaye and D. Burley, Phys. A **87**, 499 (1977).
[24] A. Ghosh, D. Dhar, and J. L. Jacobsen, Phys. Rev. E **75**, 011115 (2007).
[25] K. Froböse, F. Bonnemeier, and J. Jäckle, J. Phys. A: Math. Gen. **29**, 485 (1996).
[26] See Supplemental Material at http://link.aps.org/supplemental/10.1103/PhysRevB.95.060413 for details of the quantum trimer Hamiltonian and adjacency graph calculations.
[27] R. A. Horn and C. R. Johnson, *Matrix Analysis* (Cambridge University Press, Cambridge, U.K., 2012).
[28] L. Savary and L. Balents, Rep. Prog. Phys. **80**, 016502 (2016).
[29] P. Fendley, R. Moessner, and S. L. Sondhi, Phys. Rev. B **66**, 214513 (2002).
[30] A. Ioselevich, D. A. Ivanov, and M. V. Feigelman, Phys. Rev. B **66**, 174405 (2002).
[31] M. D. Schulz, S. Dusuel, R. Orús, J. Vidal, and K. P. Schmidt, New J. Phys. **14**, 025005 (2012).
[32] A. Kitaev, Ann. Phys. **321**, 2 (2006).
[33] R. Moessner and K. S. Raman, Quantum dimer models, in *Introduction to Frustrated Magnetism: Materials, Experiments, Theory*, edited by F. Mila, C. Lacroix, and P. Mendels (Springer, Berlin, Heidelberg, 2011), pp. 437–479 .